PAPER Nr.: 82

WIND EFFECTS ON HELICOPTER TAKE-OFF AND LANDING

BY

N.TRÄNAPP

INSTITUT FÜR FLUGMECHANIK
TECHNISCHE UNIVERSITÄT BRAUNSCHWEIG
3300 BRAUNSCHWEIG,
REBENRING 18

FIFTEENTH EUROPEAN ROTORCRAFT FORUM

SEPTEMBER 12 - 15, 1989 AMSTERDAM

WIND EFFECTS ON HELICOPTER TAKEOFF AND LANDING

N. Tränapp
Institut für Flugmechanik
Technische Universität Braunschweig
3300 Braunschweig,
Rebenring 18

Abstract

One of the most important parameters for helicopter takeoff and landing is wind. On account of direct influence on the desired flight path during takeoff and landing wind can give rise to considerable changes in power required, and is thus of significance to flight safety. Some accidents have been found to be caused by wind-interference, sometimes combined with some other causes, as for example engine-failure.

Investigations into normal takeoff and landing procedures according to FAR part 29, category A present the influence of wind on helicopter takeoff and landing and document possible endangering situations. In addition to this, problems of interaction between helicopters in terminal operations and aircraft vortex wakes are discussed.

The examinations employ several simulation models of different extension, which are briefly mentioned. These models will be verified by means of flight tests, with particular regard to power required.

This research was supported by the Deutsche Forschungsgemeinschaft under SFB 212 "Sicherheit im Luftverkehr"

Notation

a	ground coefficient or constant
A_0, A_1, A_2	polynomial coefficient
b	span width
D_0	profile drag
DL	disk loading
D_α, D_β	cyclic pitch angles at swashplate
g	inertial acceleration due to gravity
G	force of gross weight
H	height
$\bar{H}$	non-dimensional height ($\bar{H}$=H/R)
H_{SKID}	skid-height
K_G	weight coefficient
K_P	power coefficient
m	mass
P	power
P_{req}	power required
P_{Ro}	main-rotor power required
$P_{max,OEI}$	power available with one engine inoperative
q_x, q_r, q_t	axial, radial, tangential velocity of airplane vortex
r	radius
R	rotor radius
r^*	radius of vortex core
S	disk area or wing area
T	thrust
U	rotor tip speed
u, v, w	airspeed components
u_K, v_K, w_K	components of flight path velocity
$\dot{u}_{Kg}$, $\dot{v}_{Kg}$, $\dot{w}_{Kg}$	components of acceleration
u_W, v_W, w_W	components of wind velocity
$\underline{V}$, V	airspeed
$\underline{V}_K$, V_K	flight path velocity
V_m	velocity of maximum recirculation
$\underline{V}_W$, V_W	wind velocity
w_i	induced velocity at the rotor disk
x, y, z	components of position or distance
x_L	landing distance
X_p	power factor
X_R	recirculation factor
$X_{R,W}$	recirculation factor for hover in wind
z_0	roughness parameter of ground
α_{Ro}	shaft angle of attack

ρ	air density
Γ	circulation
Δ	difference, distance
ϑ_c, ϑ_s	cyclic blade angles
ϑ_0	collective blade angle
ϑ_{HR}	collective blade angle at tail rotor
ν	kinematic viscosity
ν_e	effective eddy viscosity
π	constant of circle

non dimensional velocities are related to the induced velocity at hover w_{iH} (e.g. $\overline{V}=V/w_{iH}$)

subscripts:

c	continuous
g	geodetical
H	hover
max	maximum
ref	reference

abbreviations:

AEO	All Engines Operating
CDP	Critical Decision Point
IGE	In Ground Effect
LDP	Landing Decision Point
OEI	One Engine Inoperative
OGE	Out Ground Effect
SFB	Sonderforschungsbereich
T.D.	Touch Down
T.O.	Takeoff

1. Introduction

In flight mechanics wind is a fundamental size, which may have considerable influence on security aspects when performing takeoff and landing. Accidents, resulting from incorrect consideration of wind give verification to this.

The aim of this paper is to describe wind influence on normal takeoff and landing with particular regard to power required. For that purpose a data field simulation and a six body-degree of freedom model with a quasisteady rotor simulation including flapping motion is applied. For simulating a desired flight path, the analytical model is converted into a controls calculating model for given accelerations. This model serves as anticipatory control in simulations with the analytical quasisteady model. High accuracy of performance calculation is important for investigations into helicopter takeoff and landing on account of the fact that power required has a strong influence on the flight path.

Further influence on power required at takeoff and landing results from ground effect. Hence, ground effect under wind conditions will firstly be investigated using windtunnel test data. The modified source model that has been verified for ground effect in forward flight without wind is used as a reference model. Using windtunnel data as a comparison, a simple approach is discussed, which allows for performance calculation in ground effect under wind conditions.

The investigation is restricted to wind without turbulent interference. Normal takeoff and landing simulations within a ground boundary wind profile are discussed. Particular danger can be induced by trailing vortices from heavy transport aircraft, a situation that should be taken care of for operations in a terminal area especially under instrument flight rules. As the investigation is focussed on power required, normal penetrations through the vortices are discussed, since in such a case power required changes rapidly and controls required for maintaining the flight path indicate the workload to the pilot or the autopilot.

2. Helicopter Simulation Models

Takeoff and landing are stages of flight that are subjected to flight path observance. For this reason, wind has a direct influence on controls and power required during takeoff and landing. For investigations on this domain, two different simulation models for the BO 105 CB helicopter are employed.

The data field simulation is designed for power required or flight path calculations for takeoff and landing and has been developed by CERBE and REICHERT /1/. The model consists of stationary state data shown in Figure 1 for the non-dimensional power required factor X_p, described as a function of the non-dimensional airspeed components $\bar{u}_g$ and $\bar{w}_g$. Translational accelerations, which essentially occur on takeoff and landing, can be transformed into equivalent non-accelerated states with equivalent mass and equivalent flight path angle. An example of the transformation to stationary states is indicated by a horizontally accelerated forward flight which can be transformed into a non-accelerated climb with an equivalent gross weight. Assuming that angular velocities and accelerations have insignificant influence on power required, the new stationary state has an oncoming flow and power required similar to the accelerated state, so that the data-field model can also be applied to non-stationary flight states.

A significant limitation of the data field simulation is the generalized performance calculation which does not allow for consideration of variing wind velocities at different sections of the helicopter. This is of importance in wind-field with strong gradients, as shown in Figure 2. It is necessary to take local wind velocities at the rotor disk into account in particular simulations for the penetration of trailing vortices induced by heavy airplanes.

For this purpose a six body-degree of freedom simulation model with consideration of the degree of blade flapping and provided with a quasistationary rotor /2/, is employed. The model is suitable for investigations into power required and the influence on controls. For simulating a desired flight path, the required controls can be calculated in a trim mode, which allows given velocities and accelerations to be trimmed for each point of time. Controls required from this mode can be applied as anticipatory control in simulation. This configuration in conjunction with an attitude control gives good compliance with a defined flight path as long as no disturbance, such as wind (e.g.) occurs.

If the disturbance is known already, it can be considered in the anticipatory control before simulating.

The requirements stated in FAR part 27 and part 29 /3/, /4/ demand a minimum 17-knot control capability for hover and takeoff in winds from any azimuth. In addition, control capability in wind from 0 knots to at least 17 knots (8.75m/s) must also be shown for any other appropriate maneuver in ground vicinity such as rolling takeoffs for wheeled rotorcraft. These requirements must be met at all altitudes approved for takeoff and landing.

For testing the simulation model, various wind azimuth and velocities are trimmed as shown in Figure 3. The trim points are calculated for a longitudinal airspeed range from backward u_g=-20 m/s to forward u_g=+60 m/s and for sideward wind velocities from v_{Wg}=-16 m/s to v_{Wg}=+16 m/s. Under such conditions 40% of the lateral cyclic pitch range and 50% of the longitudinal pitch range is covered by the required controls. This is nearly double the range requested by FAR Part 27 and 29. For the same crosswind the tail rotor collective blade angle requires nearly 80% of full authority as shown in Figure 4. This indicates, that with increasing crosswind firstly the tail rotor will reach boundaries of its efficiency, a case which might be of importance to maneuvers at low heights in surroundings with obstacles.

3. Wind Influence on Ground Effect

The consideration of ground effect is essential for investigations into takeoff and landing, because ground effect has a remarkable influence on power required during takeoff or landing-sections in ground effect-heights between H/R=0.8 and H/R=1.2 (that means skid-heights from H_{SKID}=1m÷3m).

An appropriate, relatively simple formulation for power required, dependant on ground effect height, is the source Model of CHEESEMAN and BENNETT /5/ outlined in Figure 5. Their main assumption uses a source-flow-model from potential theory for the rotor downwash at low heights above ground. The surface-induced deflection of streamlines is attained by a second source of equal strength lying below the surface at the same distance as the rotor-source. Thereby no streamline penetrates the ground-surface. The source-model includes the influence of forward velocity on power required under the assumption of small rotor disk angles α_{Ro}. The relation of the rotor induced velocity for in ground effect (IGE) and out ground effect (OGE) results from source model assumption for constant thrust:

Source Model:

$$\left(\frac{w_{i,IGE}}{w_{i,OGE}}\right)_{T=const} = \left[1 - \frac{1}{16} \cdot \left(\frac{1}{\bar{H}}\right)^2 \cdot \left(\frac{w_{i,OGE}}{w_{iH,OGE}}\right)^4\right]^{\frac{3}{2}} \qquad (3.1)$$

This approximation depends on non-dimensional ground effect height $\bar{H}$=H/R and on the rotor induced velocity in hover for out ground effect (OGE) $w_{iH,OGE}$. This relation can be extended to the relation of the rotor-induced power for in ground effect (IGE) and out ground effect (OGE) with premise of momentum theory:

Momentum Theory:

$$\left(\frac{w_{i,IGE}}{w_{i,OGE}}\right)_{T=const} = \left(\frac{P_{i,IGE}}{P_{i,OGE}}\right)_{T=const} \qquad (3.2)$$

The source model has been compared with flight test results and shows good consistency with measuring values for hover in various ground effect heights.

However, in forward flight at low advance ratios, the power required calculation from the source model is estimated too low on account of insufficient consideration of the ground vortex which is represented in Figure 6. For low velocities in ground effect the rotor-induced downwash builds up rotational wave, which surrounds the helicopter like a horseshoe. In the outer front area of the rotor disk, the vortex induces a recirculation flow, which supports a rise in induced power required for low forward speed in ground effect (IGE).

With increasing forward speed the ground vortex moves nearer to the helicopter, and the recirculation in the efficient outer disk plane is converted into an upwash below the front rotor area, which reduces power required.

These effects initially have been investigated by CURTISS /6/ by means of a model rotor in a special tracking facility, which enables the rotor to move through still air. Contrary to windtunnel tests, CURTISS's investigations represent the ground boundary condition for forward flight in ground effect without wind.

CURTISS's experimental research provided information regarding the influential sphere of the recirculation and the power required reducing ground vortex region. The Figure 7 shows the boundaries found during CURTISS'S flow visualization studies.

CERBE, CURTISS and REICHERT /7/ determined a linear equation $\bar{V}_m(\bar{H})$ under the assumption, that the maximum recirculation effect can be found in the middle of the recirculation area. The approximation for the non-dimensional velocity of maximum recirculation $\bar{V}_m$ as a function of non-dimensional height is given as:

$$\begin{aligned} &\underline{\text{Velocity of Maximum Recirculation:}} \\ &\underline{\bar{H} < 3{,}5:}\ \ \bar{V}_m = 0{,}72 - 0{,}206 \cdot \bar{H} \\ &\underline{\bar{H} \geq 3{,}5:}\ \ \bar{V}_m = 0{,}0 \end{aligned} \tag{3.3}$$

In the modified source model by CERBE, CURTISS and REICHERT /7/ the influence of ground vortex on the induced main rotor power for in ground effect (IGE) and out ground effect (OGE) is taken into account by the recirculation factor X_R:

$$\underline{\text{Modified Source Model:}}$$

$$\left(\frac{P_{i,IGE}}{P_{i,OGE}} \right)_{T=const} = \left[1 - \frac{1}{16} \cdot \left(\frac{1}{\bar{H}} \right)^2 \left(\frac{w_{i,OGE}}{w_{iH,OGE}} \right)^4 \cdot X_R \right]^{\frac{3}{2}} \tag{3.4}$$

The variation of the recirculation factor for the non-dimensional velocity is assumed by a quadratic equation:

$$\underline{\text{With Recirculation Factor } X_R:}$$

$$\underline{\bar{V}_m > 0:}\ \ X_R = 1 - 2 \cdot X_{R,max} \cdot \left(\frac{\bar{V}}{\bar{V}_m} \right) + X_{R,max} \cdot \left(\frac{\bar{V}}{\bar{V}_m} \right)^2$$

and

$$\underline{\bar{V}_m = 0:}\ \ X_R = 1 \tag{3.5}$$

The factor $X_{R,max}$ describes the effect of variations of the relation $(\bar{V}/\bar{V}_m)$ and $(\bar{V}/\bar{V}_m)^2$ on the recirculation region.

The modified source model has been well approved for power required calculation in forward flight for in ground effect following flight tests conducted by LIESE, RUSSOW and REICHERT /8/. These flight tests, performed at wind velocities V_{Wg} lower than 1 m/s, indicate a maximum recirculation factor $X_{R,max}$=0.5, which can be obtained for the ground effect without wind, resulting from translational motion of the helicopter only.

By taking wind into consideration an influence of the changed ground boundary on ground effect and power required can be assumed. Figure 8 outlines the situation at translational motion without wind and at hover in a horizontal wind-field. On account of ground boundary in the case of wind, the superposition of oncoming flow and rotor-induced horizontal velocity indicates an increasing shear flow in the resultant horizontal velocity. Since the ground vortex is induced by the shear flow, it is supposed to have more circulation strength in a given horizontal wind situation than without wind.

To investigate the wind influence on power required,flight tests under wind conditions or windtunnel tests are appropriate. Early research work conducted by JENSEN /9/ on shelterbelts shows, that the boundary layer in a windtunnel can be similar to the boundary layer induced by horizontal wind. SHERIDAN and WIESNER /10/ have conducted windtunnel tests with a 120-SHP-model for the Boing-Vertol YUH-61 A - helicopter.

The increase in main rotor power required in the recirculation regime is a particulary important result of the investigations. At low disk loading the recirculation in a non-dimensional height H=0.8 is measured as being even higher than in the case of out ground effect (OGE). Figure 9 shows the non-dimensional main rotor power measured by SHERIDAN and WIESNER and the calculation for the modified source model for in ground effect (IGE) and out ground effect (OGE) at a disk loading DL=8PSF. The smooth rise in main rotor power out ground effect (OGE) can be reduced to the effect of windtunnel walls, which may cause a slight recirculation flow at low velocities.

As the measurements have been plotted for the main rotor power, they can be suitable compared in nondimensional form with results from the source model, which is based on assumptions of momentum theory.

Conclusions as to wind influence on the ground effect can be obtained from the difference between the out ground effect (OGE) and in ground effect (IGE) curve for the windtunnel data and on the other hand from the calculation by the modified source model. The difference functions are described in Figure 10. The calculation from the modified source model, which is assumed to represent the translational motion of the helicopter without wind, is performed for a maximum recirculation factor $X_{R,max}$=0.5 which has been established by means of flight tests with low wind velocities by CERBE, CURTISS and REICHERT /7/. On the other hand the windtunnel test data corresponds to the wind situation.

The additional traced variation between both curves indicates that for low velocities the recirculation effect at hover in wind is higher than in translational motion without wind. With increasing velocities, however, the power required reducing ground vortex enables greater power reduction in the case of wind, than in pure rigid body movement without wind.

Comprehensive comparison with the windtunnel investigation conducted by SHERIDAN and WIESNER /10/ confirms the assumption of increasing ground vortex circulation strength for hover in wind.

As the influence of wind on ground effect results from ground vortex, the recirculation factor X_R from the modified source model can be used for adjusting the modified source model to deliver correct main rotor power calculation in respect of wind. A simple appropriation for the recirculation factor in wind $X_{R,W}$ from the modified source model is:

Recirculation Factor for Hover in Wind X_{RW}:

$$\underline{\bar{V}_m > 0:} \quad X_{RW} = 1 - X_{R,max,W} \cdot \left(\frac{\bar{V}}{\bar{V}_m} \right) \qquad (3.6)$$

$$\underline{\bar{V}_m = 0:} \quad X_{RW} = 1$$

A maximum recirculation factor in wind of $X_{R,max,W}$=1.0 renders good consistency of measuring and calculated values for low velocities in Figure 11. Unfortunately the set up with $X_{R,max,W}$=1.0 does not match for the whole range of velocity. For this reason an optimization of the maximum recirculation factor in wind $X_{R,max,W}$ has been performed and is plotted in Figure 12 as a function of non-dimensional velocity $\bar{V}$. Value $X_{R,max,W}$=0 represents the calculation from the source model by CHEESEMAN and BENNETT /5/.

Values higher than $X_{R,max,W}$=0 indicate an increase of power required compared to the source model, values smaller than $X_{R,max,W}$=0 indicate decreasing power required.

In order to investigate the influence of wind on total power required and to compare calculated and measured total power required from the flight test, transfer to non-dimensional parameter is required.

To reduce the influence of mass m and atmospheric conditions on power required P_{req}, LIESE, RUSSSOW and REICHERT /8/ apply the power coefficient K_P:

Power Coefficient:

$$K_P = \frac{2 \cdot P}{\rho \cdot U^3 \cdot S} \tag{3.7}$$

and the weight coefficient K_G:

Weight Coefficient:

$$K_G = \frac{2 m \cdot g}{\rho \cdot U^2 \cdot S} \tag{3.8}$$

The power coefficient for hover can be separated into the weight-independant term $K_{PH}(K_G=0)$ and the term ΔK_{PH} which takes weight influence into account:

Power Coefficient for Hover:

$$K_{PH} = K_{PH}(K_G=0) + \underbrace{A_1 \cdot K_G + A_2 \cdot K_G^2}_{\Delta K_{PH}(K_G)} \tag{3.9}$$

A_1, A_2: Regression-Coefficients Estimated from Flight Test Data

a power factor X_P for forward flight can be defined:

Power Factor for Forward Flight:

$$X_P = \frac{K_P(K_G, \bar{V}) - K_{PH}(K_G=0)}{\Delta K_{PH}(K_G)} \tag{3.10}$$

The power factor is well suitable for comparison between flight test data and calculation results.

Figure 13 shows data from the flight test conducted with a BO 105-Helicopter and results from calculations with different ground effect models for a non-dimensional height $\bar{H}$=0.8 corresponding to a skid-height H_{SKID}=1.0 m. The measurements out ground effect (OGE) are represented only by a regression-curve. The measurements in ground effect (IGE) apply to the case of rigid body movement as all data have been measured at wind-velocities lower than 1 m/s. Performance calculation using the modified source model gives the best accommodation to these data. Complementary performance calculation with the approach taking wind into account is plotted under the assumption, that airspeed results only from wind velocity.

At hover for takeoff, power required will be higher in a ground boundary induced wind profile up to wind-velocities of about 10 m/s. Under the same conditions a decrease in the power required reducing ground cushion-effect should be taken into account at landing. The abrupt change in power required in the transition region between ground vortex and recirculation regime may especially cause rapid changes in power required when airspeed in ground effect varies only slightly.

Figure 14 for ground height $\bar{H}$=1.0 indicates the decrease of wind influence on power required with increasing height.

In the following the influence on takeoff and landing will be described for selected examples.

4. Takeoff and Landing in Consideration of Wind

Helicopter Takeoff and Landing procedures are covered by the Federal Aviation Regulations Part 27 for helicopters with gross weight up to 2700 kg (6000 lbs.) and in Part 29 for multiengine helicopters. Part 29 is separated into Category B valid for single- or multiengine helicopters with a gross weight limitation of 9000 kg (20000 lbs.) and non-independent engines, and Category A, which determines requirements for procedures with engine failures during takeoff and landing for helicopters with unlimited gross weight and independent engines.

Figure 15 illustrates the normal takeoff with and without power excess. The height loss for takeoff without power excess results from ground effect. AEO means: All Engines Operating, OEI means: One Engine Inoperative. After acceleration in ground effect to the decision speed V_{CDP}, the helicopter passes over into the climb segment. The takeoff distance x is attained, when a height of H=50ft with the velocity V_Y for maximum rate of climb is passed.

The critical decision point CDP characterizes a height H_{CDP} and a velocity up to which point a takeoff has to be rejected, if an engine failure occurs. The rejected takeoff distance x is measured, if ground-velocity V_K=0 m/s is attained. Engine failure after CDP requests a continued takeoff with one engine emergency power $P_{max,OEI}$ and a minimum climb-rate of 100 ft/min (0.5m/s), which is available at the takeoff safety airspeed V_{TOSS}. If V_{CDP} is greater than or equal to V_{TOSS}, the climb can be continued, if V_{CDP} is less than V_{TOSS}, the acceleration to V_{TOSS} with a height loss not beyond $H_{min} > H_{CDP}/2$ is allowable. The continued takeoff distance x is measured for reaching a height of H=35ft and the takeoff safety speed V_{TOSS}. The required takeoff distance is regarded as the greater of the distances of continued takeoff and rejected takeoff.

The distance x_L for the conventional landing is the horizontal length x_L from the point, at which a height of H_{xL}=50 ft above the landing surface is passed in descent, to the point that marks the standstill on the ground. The landing decision point characterizes a height H_{LDP} that renders a balked landing with acceleration to the takeoff safety speed V_{TOSS} at an altitude no lower than H=35 ft above the landing surface, if an engine failure occurs in the LDP. A typical LDP-height H_{LDP} for conventional landings is 100 ft above the ground. In the approach prior to the LDP, with one engine inoperative, the balked landing as well as the continued landing are possible profiles. Engine failures beyond the LDP-height require a continued landing.

For the investigation into the influence of wind on helicopter takeoff and landing a simple approach for the PRANDTL-ground boundary /11/ for the horizontal wind velocity $u_{Wg}(H)$ is assumed:

Horizontal Wind Velocity:

$$u_{Wg}(H) = u_{Wg,ref} \cdot \left(\frac{H}{H_{ref}}\right)^{a} \qquad (4.1)$$

The reference wind velocity $u_{Wg,ref}$ is measured at the reference height H_{ref}=10 m, which characterizes the thickness of the boundary layer on the ground for horizontal wind. Within the ground boundary the wind velocity increases to up to 99% of the total amount. The ground coefficient a decreases with growing height H, though since this investigation is focused on small heights H only, the coefficient for the surface-roughness is assumed to be constant:

Ground Coefficient a:

$$a = \frac{1}{\ln\left(\frac{H_{ref}}{z_0}\right)} \qquad \begin{array}{ll} \text{Sand:} & a = 0{,}14 \\ \text{Low Grass:} & a = 0{,}3 \\ \text{High Grass:} & a = 0{,}4 \end{array} \qquad (4.2)$$

Figure 16 describes the horizontal wind profiles in the ground boundary for various surface-roughnesses. Since the continued takeoff and the balked landing are performed out of the boundary layer, this investigation does not treat the influence of wind on the balked landing and on the continued takeoff.

A vertical descent shown in Figure 17 with given constant power P and a vertical velocity of w_{Kg}=1m/s in variable head wind reference velocities $-u_{Wg,ref}$ gives good insight as the influence of wind on the ground effect can be obtained by means of the touch down velocity $w_{Kg,T.D.}$. On the one hand, the increase of the touch down velocity $w_{Kg,T.D.}$ depends on the reduction of the wind velocity $-u_{Wg}$ within the ground boundary layer, on the other hand the touch down velocity depends on the ground effect model.

The calculation with the modified source model in consideration of wind indicates the greatest rise in the touch down velocity $w_{Kg,T.D.}$. In the range of higher head wind velocities $-u_{Wg,ref}$ the ground vortex in consideration of wind has a reducing influence in the increase of the touch down velocity $w_{Kg,T.D.}$, corresponding to the variation of power required P_{req}. Additionally, the modified source model in consideration of wind has been calculated with a time delay for the building up of the ground vortex. This approximation has been set up by CERBE, CURTISS and REICHERT /7/, and will be used for the following investigations.

A characteristic approach-profile, calculated by the data field simulation model with one engine inoperative, is shown in Figure 18, for the case of no wind.

The horizontal and vertical approach velocity components u_{Kg} and w_{Kg} in the 50 ft-height at x_L=0 m are fixed given handicaps for each wind velocity,assuming that terminal operation rules require a defined flight path. The slopes for the accelerations $\dot{u}_{Kg}$ and $\dot{w}_{Kg}$ have been found by an optimization algorithm which minimizes the landing distance x_L.

A significant decrease in power required, almost as much as P_{req}=0 kW, occurs when the flare-segment is initiated. CERBE and REICHERT /1/ found, that for optimization purposes it is favourable to increase and immediately to decrease the vertical acceleration $\dot{w}_{Kg}$ in the flare-segment with a permitted gradient.

The acceleration $\dot{u}_{Kg}$ for the flare-segment is optimized in such a way, that the rise in the power required P_{req} does not require more variation than P_{req}=80 kW/s /1/. If the acceleration have reached a suitable amount for the variation in power required P_{req}, it is held constant. The vertical acceleration $\dot{w}_{Kg}$ then depends only on the requirement to reach a horizontal velocity w_{Kg}=0 m/s at a low given height above the ground. If the horizontal velocity u_{Kg}=0 m/s cannot be attained the horizontal acceleration $\dot{u}_{Kg}$ is constant until power required P_{req} reaches the emergency power for one engine inoperative $P_{max,OEI}$ and the touchdown on the ground occurs. From that point on, the remaining velocity is reduced by a simple friction approximation, which calculates a constant horizontal acceleration.

Figure 19 describes the influence of wind on power required P_{req} in the flare-segment, if the flight path from the optimization for the case of no wind is maintained under wind conditions.

With increasing horizontal head wind velocity $-u_{Wg}$ the rise in power required P_{req} in the flare-segment is reduced. This indicates, that the horizontal acceleration $\dot{u}_{Kg}$ can be higher and thus the landing distance x_L under head wind conditions can be reduced.

The wind influence on the rejected takeoff can be considered in Figure 20. The takeoff profile begins at a height of $H_{T.O.}$=1 m with a horizontal acceleration $\dot{u}_{Kg}$ which induces a rise in power required and considers the time response of the drive unit.

Contrary to landing requirements, the takeoff procedure is aligned to the airspeed V. For this reason, the horizontal acceleration $\dot{u}_{Kg}$ for the simulation under wind velocity $u_{Wg,ref}$=10 m/s decreases rapidly and the climb can be initiated. The engine failure occurs in the CDP at the same height H_{CDP} as in the case of no wind.

The optimization algorithm found that slight horizontal deceleration $\dot{u}_{Kg}$ following the engine failure shortens the distance x for the rejected takeoff, since the decrease in power required P_{req} in the flare segment becomes smaller. Of course, the takeoff distance x is considerably influenced by horizontal head wind.

Figure 21 gives a general view of the influence of wind on the takeoff or respectively landing distance x or x_L. No significant influence of wind on the landing distance is evident due to the fact, that it is necessary to keep a given flight path, according to landing and terminal requirements.

Contrary to this, takeoff distance depends considerably on the horizontal wind velocity u_{Wg}. In addition, the influence of gross weight on the takeoff distance diminishes with increasing wind velocity, on account of a decrease in the required horizontal acceleration.

The broken line for the rejected takeoff at the gross weight for m=2300 kg indicates, that the assumed optimization algorithm did not succeed in finding for a solution to satisfy the preassumed condition of reaching the vertial velocity w_{Kg}=0 m/s at the touch down point. This is caused by the increase in power required which is induced by the ground effect for decreasing wind velocities u_{Wg} within the ground boundary.

Another influence of wind on takeoff and landing is caused by the interaction between aircraft vortices and helicopters in the terminal area, which is described in the following.

5. Interaction between Aircraft Vortices and Helicopter

During takeoff and landing in terminal area the wind phenomenon of vortex wakes from heavy aircraft represents an additional influence of wind on helicopters. Certainly, the interference range of vortices is only of local extent and depends on time, the wake-system may have extraordinarily strong gradients of wind velocity changes. In crosswind conditions, trailing vortices can drift across the ground and reach adjoining runways or hovering helicopters. Measurements conducted by PENGEL and TETZLAFF /12/ at the Frankfurt Rhein-Main airport indicate that a crosswind-velocity higher than 4.5 m/s enables the wake-system to cover a distance of 518 m to the next runway.

A characteristic situation for terminal operations is described in Figure 22. In addition, the vortex-induced vertical wind velocity-profile for a longitudinal distance of Δx =-4000 m from the vortex-generating airplane is represented. In this investigation only normal vortex-penetrations by a helicopter are considered, since this demands rapid change in controls and in power required. The model for the airplane wake, also used by SAITO /13/, is based on assumptions by LAMB /14/, representing the solution to the NAVIER-STOKES-equation for a three dimensional, viscous vortex:

Circulation:

$$\Gamma = \underbrace{\frac{4 \cdot L}{\pi \cdot \rho \cdot V \cdot b}}_{\Gamma_0} \cdot \sqrt{1 - \left(\frac{2y}{b}\right)^2}$$

Axial Velocity:

$$q_x = -\frac{D_0}{4 \cdot \pi \cdot \rho \cdot V_e \cdot x} \cdot e^{-\left(\frac{r}{r^*}\right)^2}$$

Radial Velocity:

$$q_r = -\frac{D_0}{2\pi \cdot \rho \cdot V \cdot x \cdot r} \cdot e^{-\left(\frac{r}{r^*}\right)^2}$$

Tangential Velocity:

$$q_t = \frac{\Gamma_0}{4 \cdot \pi \cdot x} \sqrt{\frac{V \cdot x}{V_e}} \cdot \left(\frac{r^*}{r}\right) \cdot \left(1 - e^{-\left(\frac{r}{r^*}\right)^2}\right)$$

With Radius of Vortex Core:

$$r^* = \frac{2 \cdot x}{\sqrt{\frac{V \cdot x}{V_e}}}$$

Effective Eddy Viscosity:

$$V_e = V + a \cdot \Gamma_0 \qquad (a \approx 0{,}0002 \div 0{,}002)$$

Data for the Vortex-Generating B 747			
Span Width	b	59,6	m
Wing Area	S	511,0	m^2
Airspeed	V	94,4	m/s
Gross Weight	m	$3{,}51 \cdot 10^5$	kg
Profile Drag	D_0	$49{,}0 \cdot 10^3$	N
Kinematic Viscosity	v	$1{,}464 \cdot 10^{-5}$	m^2/s

The three components of the velocity can be expressed as components of the wind velocity V_{Wg} by means of a transformation from polar coordinates to rectangular coordinates. The data for the vortex generating B747 airplane can be obtained from the table. These equations describe the wake, shown in Figure 23 for the induced vertical velocity w_{Wg}. The wake model is not valid for the area very close behind the airplane, where the trailing vortices have not yet completely formed.

On account of the strong variation in wind velocity, the helicopter model, which takes into account local wind velocities at each segment of the rotor disk plane, is applied for the simulation of the penetration into a wake system. As the investigation is focussed on power required, normal penetrations through the trailing vortices have been simulated since in such a case power required changes rapidly. This is shown in Figure 24 for a normal penetration of trailing vortices during helicopter takeoff for a distance of Δx=-4000 m from the airplane. The core centre of the wake system is located at a height of H=10 m. After reaching the takeoff safety speed V_{TOSS}=16 m/s at the non-dimensional height $\bar{H}$=0.8 , the helicopter turns into climb and crosses beyond the left and above the right vortex core centre. On account of the climb section, the helicopter does not hit the core centres exactly, and therefore two peaks in head wind v_{Wg} at the helicopter centre of gravity occur. Since the vertical load factor n_{zf} changes only slightly during the vortex penetration, flight path restraint in simulation is evident. In this case the steep rise in power required P_{req}, to a higher level than the maximum continuous power $P_{max,c}$ indicates, that the desired flight path from the simulation cannot be followed, which might cause endangering situations for low level flying helicopters and during takeoff and landing.

The required controls transfer an exceptional workload onto the pilot or at least onto the automatic control system. It is noticeable, that the requested change in the cyclic blade angle ϑ_c on passing the left vortex core has been limited by the maximum velocity of the actuators, and that no delaying pilot reaction is assumed in the calculations.

Good insight as to the influence of the distance Δx from the wake-generating airplane can be obtained for normal penetration into the vortices from Figure 25. Even at a distance of Δx=-20 km a remarkable change in power required occurs. However, it should be indicated, that an extrapolation to wider distances is not permissible on account of the maximum durability of the vortices in the range of 200 sec to 300 sec.

6. Conclusion

The influence of wind on helicopter takeoff and landing has been shown for a few selected situations by means of simulation models. In particular the ground effect, which can have considerable influence on the power required, has been examined under wind conditions by means of windtunnel tests and flight test data. The stronger circulation of the ground vortex in wind induced ground boundary layer, gives rise to an increase in power required for hover in low horizontal wind velocities and a decrease in power required for hover in the so called ground vortex regime.

The simulations for optimized takeoff and landing indicate that the landing distance is practically independent of the wind situations, since the approach is assumed to be performed under terminal requirements with a defined flight path and constant ground speed.

On the other hand, the distance for normal takeoff and rejected takeoff indicates a considerable variation for different head wind velocities. This result is due to the fact, that takeoff requirements are aligned to the airspeed. Constant airspeed carries to decreasing ground speed if the head wind component increases. In this case the influence of the gross weight on the takeoff distance diminishes, since the required horizontal acceleration of the helicopter mass decreases.

The short view on the interaction between aircraft vortices and helicopters indicates possible endangering situations for helicopters in the terminal area. Vortices induced by heavy transport aircraft can give rise to considerable changes in power required, which indicates, that a takeoff-flight path cannot be followed. The required controls for the normal penetration case show that the workload passed onto the pilot or at least onto the automatic control system can reach an extraordinary level.

7. References

/1/ T. Cerbe, G. Reichert, Optimization of Helicopter Takeoff and Landing, ICAS-Paper, ICAS-88-6.1.2, 16th ICAS-Congress, (International Council of the Aeronautical Sciences) Jerusalem, 1988

/2/ U. Arnold, Entwicklung eines Hubschraubersimulationsprogramms, DGLR-Jahrestagung, Vortrag-Nr. 087-123, Berlin, Germany, 1987

/3/ U.S. Department of Transportation, Federal Aviation Administration, Federal Aviation Regulations, Part 27-Airworthiness Standards: Normal Category Rotorcraft, 1972

/4/ U.S. Department of Transportation, Federal Aviation Administration, Certification of Transport Category Rotorcraft, Advisory Circular, AC 29-2, 5/20/1983

/5/ I.C. Cheeseman, W.E. Bennett, The Effects of the Ground on a Helicopter Rotor in Forward Flight, AAEE Report, Reports and Memoranda No. 3021, Sept. 1955

/6/ H.C. Curtiss Jr., M. Sun, W.F. Putman, E.J. Hanker, Rotor Aerodynamics in Ground Effect at Low Advance Ratios, 37th AHS (American Helicopter Society) Forum, 1981

/7/ T. Cerbe, G. Reichert, Influence of Ground Effect on Helicopter Takeoff and Landing Performance, 14th ERF (European Rotorcraft Forum), Milano, Italy, Sept. 1988

/8/ K. Liese, J. Russow, G. Reichert, Correlation of Generalized Helicopter Flight Test Performance Data with Theory, 13th ERF (European Rotorcraft Forum), Arles, France, Sept. 1987

/9/ M. Jensen, The Model Law for Phenomena in Natural Wind, Ing.-Internat. Edit., 2, No. 4 pp. 121-128

/10/ P.F. Sheridan, W. Wiesner, Aerodynamics of Helicopter Flight Near the Ground, 33th AHS (American Helicopter Society) Forum, May 1977

/11/ L. Prandtl, Bericht über die Untersuchungen zur ausgebildeten Turbulenz, Zeitschrift für angewandte Mathematik und Mechanik 5, 136, 1925

/12/ K. Pengel, G. Tetzlaff, Vermessung von Wirbelschleppen mit Anemometern am Flughafen Frankfurt/-Main, Abschlußbericht zu Vorhaben Nr. L-4/83-50050/83 des BMV, Hannover 1985

/13/ S. Saito, A. Azuma, Y. Okuno, T. Hasegawa, Numerical Simulations of Dynamic Response of Fixed and Rotary Wing Aircraft to a Large Airplane Wake, 13th ERF (European Rotorcraft Forum), Arles, France, Sept. 1987

/14/ H. Lamb, Hydrodynamics, Fifth Edition, Cambridge, University Press 1924,

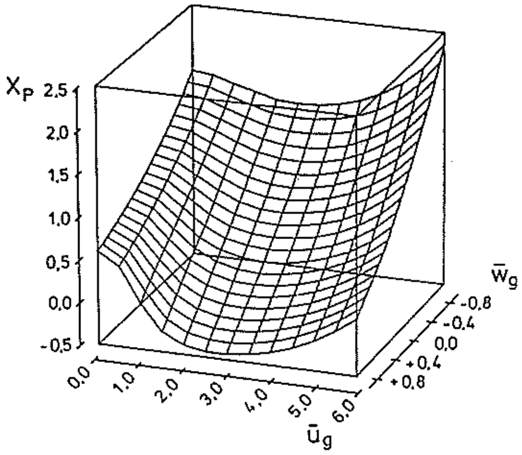

Figure 1: Power Factor at Forward Flight with Climb/Descent

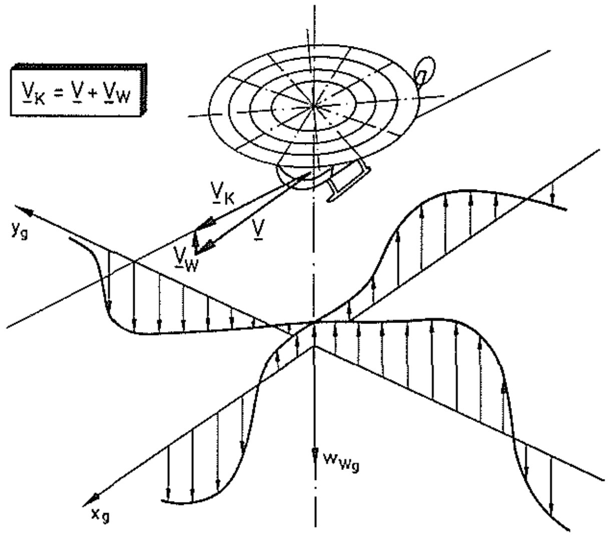

Figure 2: Penetration of a Vertical Wind Field with Varying Wind-Velocity

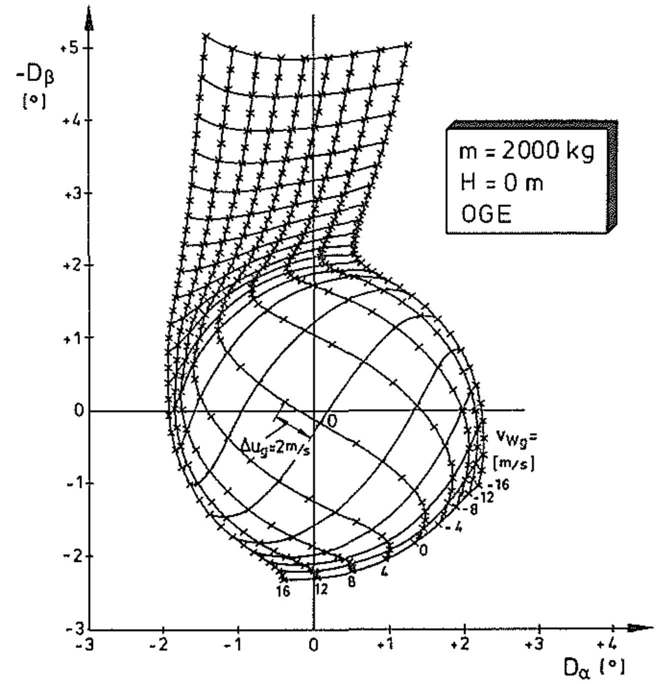

Figure 3: Cyclic Pitch Angle at Swashplate as Function of Airspeed

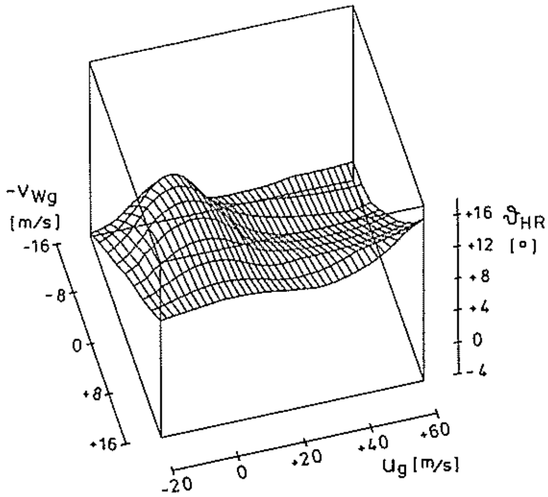

Figure 4: Tail Rotor Collective Blade Angle as Function of Airspeed

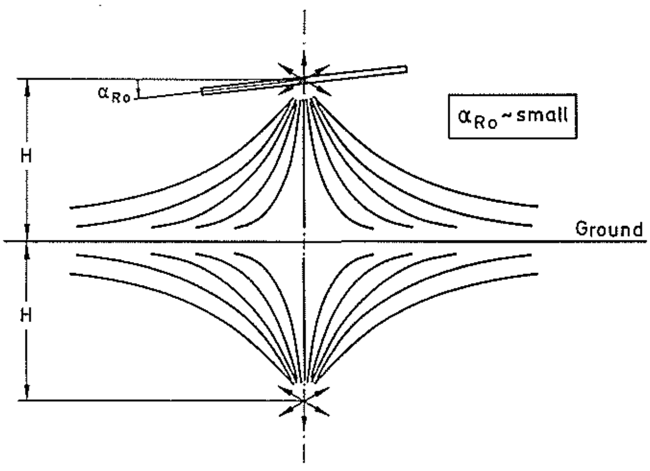

Figure 5: Source Model in Ground Effect

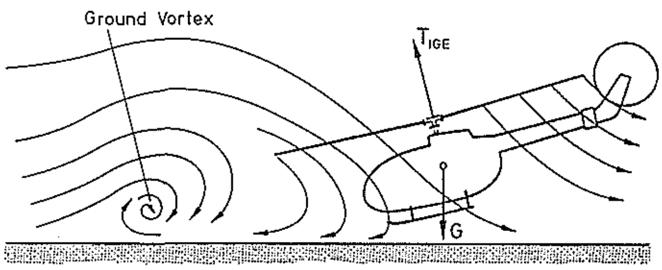

Figure 6 : Helicopter in Ground Effect for Low Forward Speed

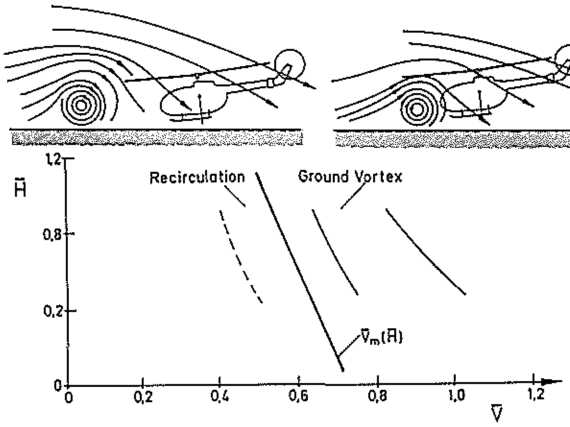

Figure 7: Boundary for Recirculation and Ground Vortex Regions

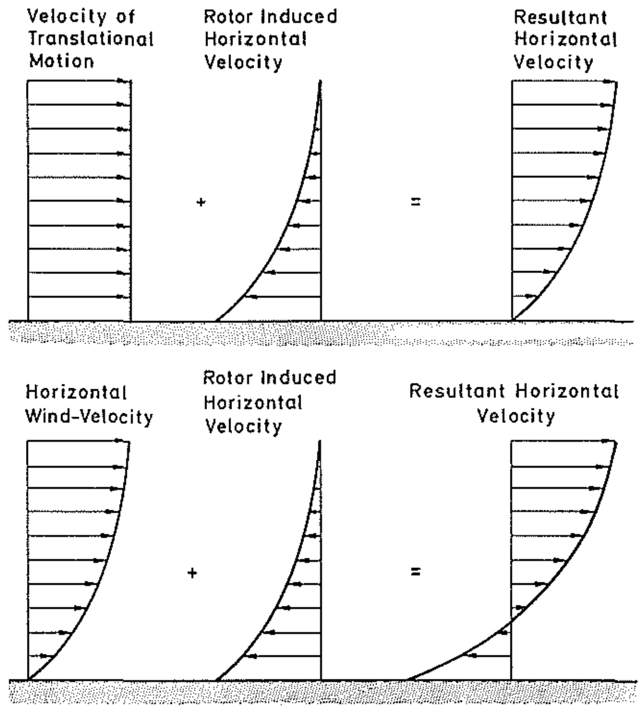

Figure 8: Resultant Horizontal Velocity in Ground Effect in Case of Translational Motion and Wind

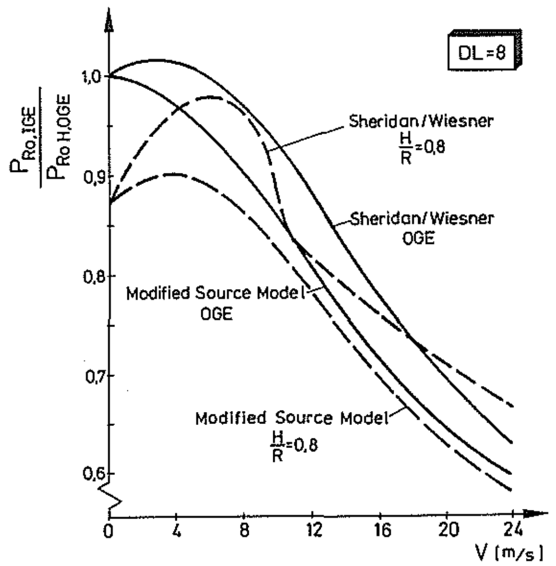

Figure 9: Non-Dimensional Main Rotor Power Required in Ground Effect

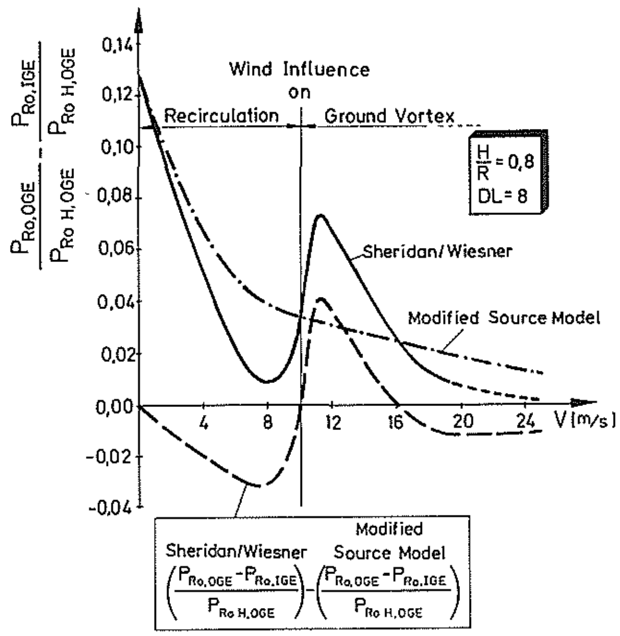

Figure 10: Non-Dimensional Main-Rotor-Power-Required-Difference between OGE- and IGE-Case

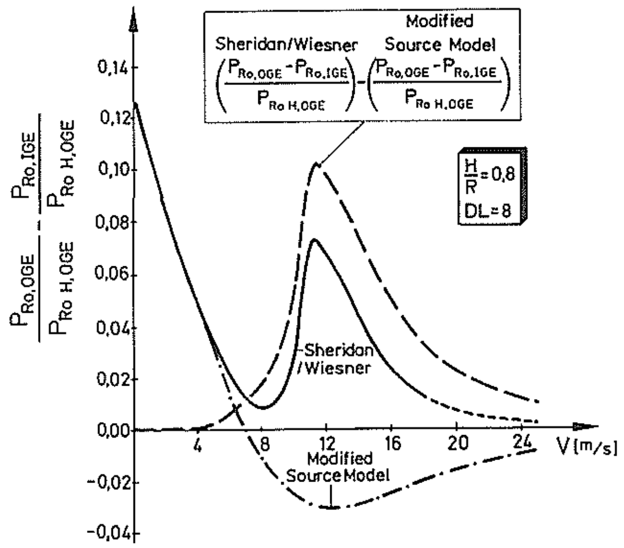

Figure 11: Non-Dimensional Main-Rotor-Power-Required-Difference between OGE- and IGE-Case

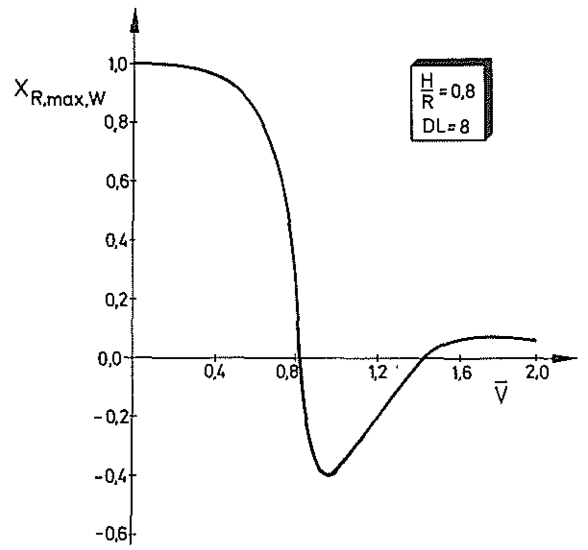

Figure 12: Maximum Recirculation Factor in Case of Wind

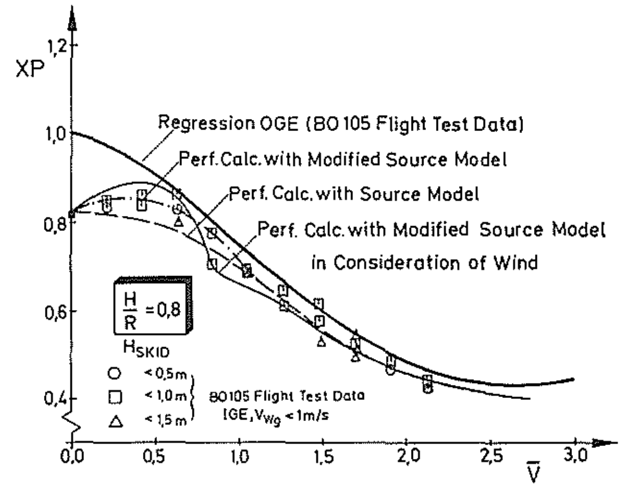

Figure 13: Influence of Ground Effect on Power Factor in Forward Flight

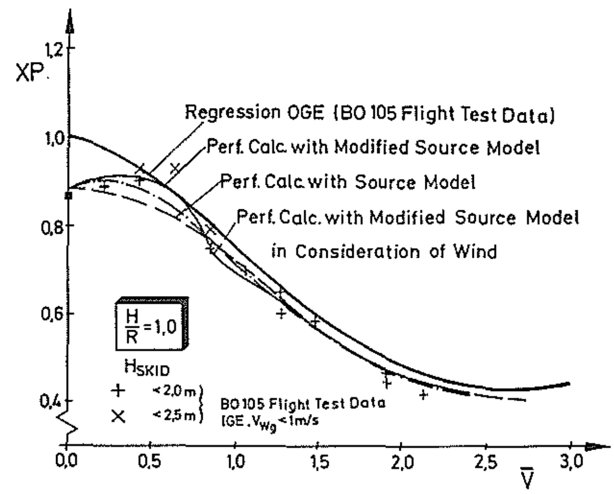

Figure 14: Influence of Ground Effect on Power Factor in Forward Flight

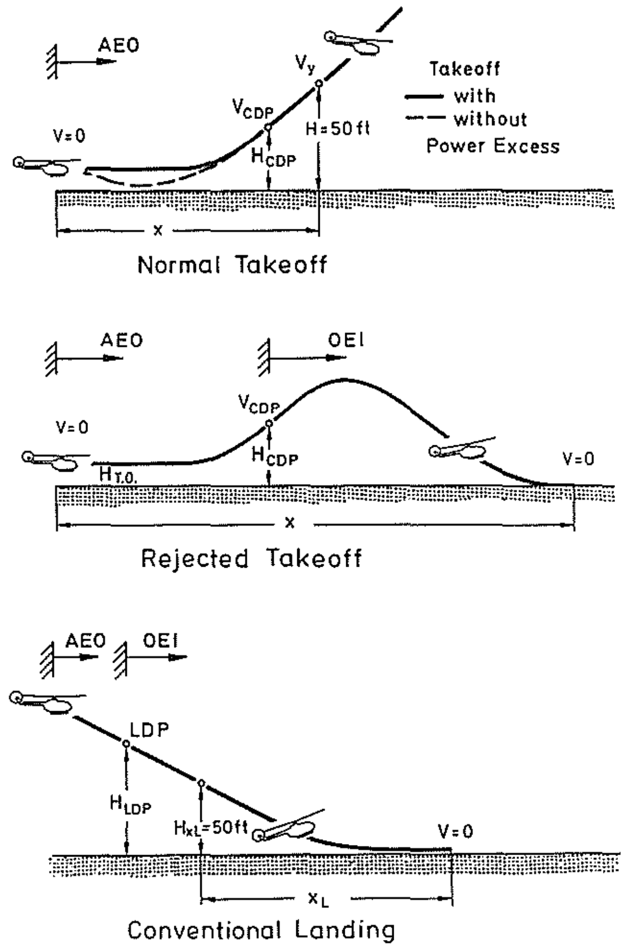

Figure 15: Takeoff- and Landing Profiles

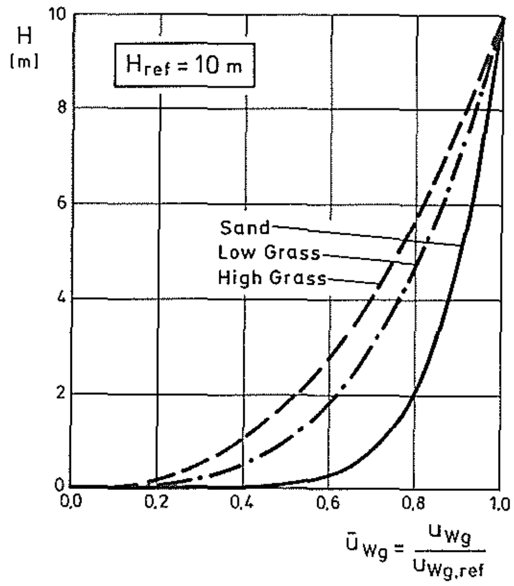

Figure 16: Non-Dimensional Horizontal Wind-Velocity as Function of Height and Surface-Roughness

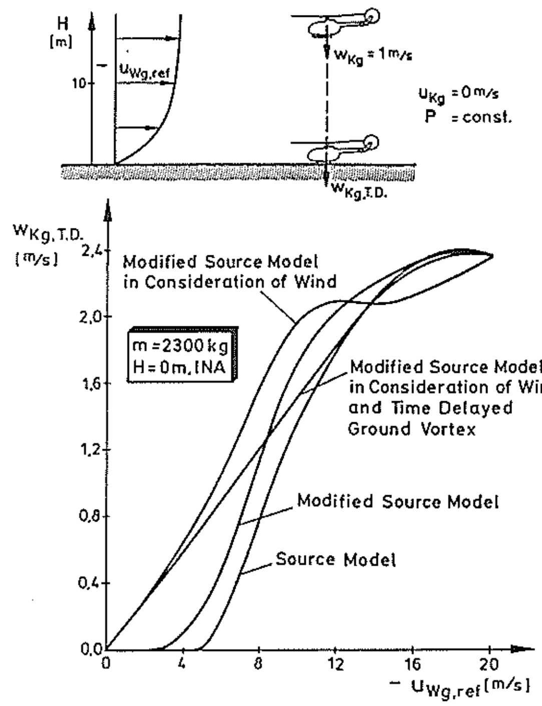

Figure 17: Influence of Ground Boundary Layer on Vertical Velocity at Touch Down for Descent (P = const.)

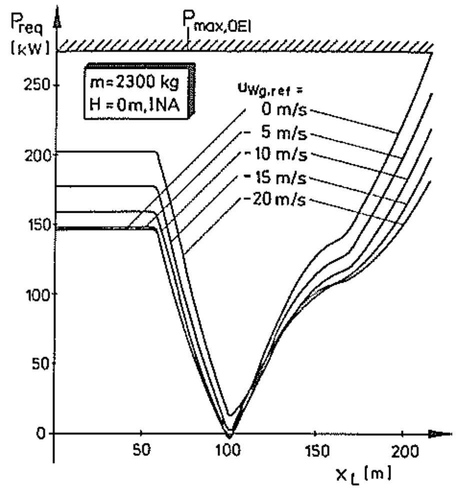

Figure 19: Power Required in Flare-Segment for Defined Flight Path

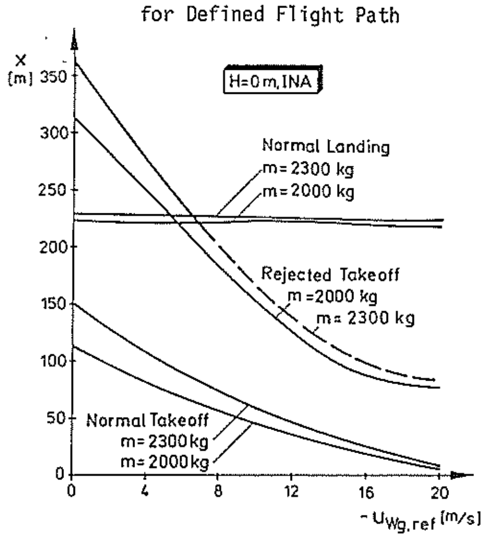

Figure 21: Wind Influence on Takeoff and Landing Distance

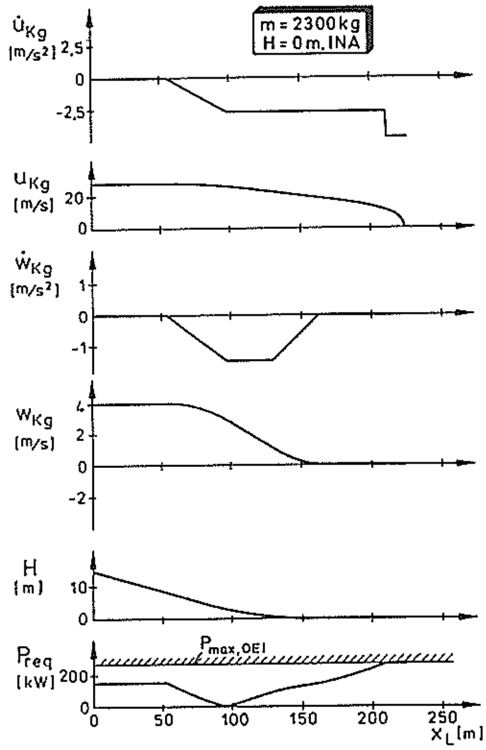

Figure 18: Approach with One Engine Inoperative (u_{Wg}=0m/s)

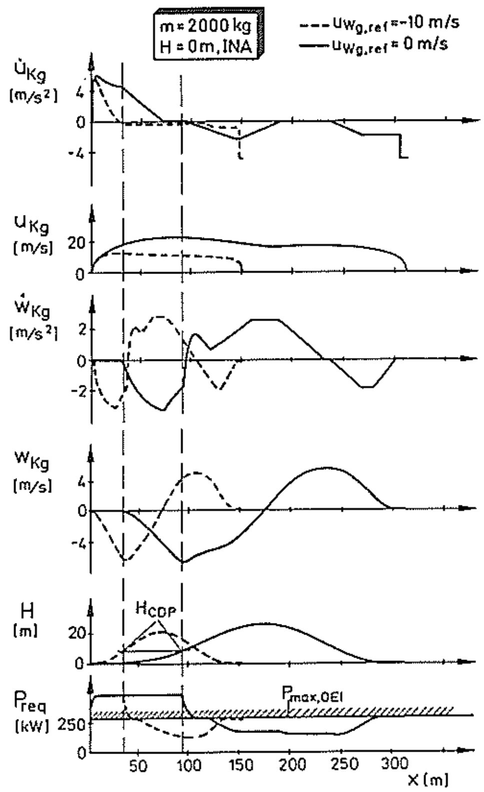

Figure 20: Wind Influence on Rejected Takeoff-Profile

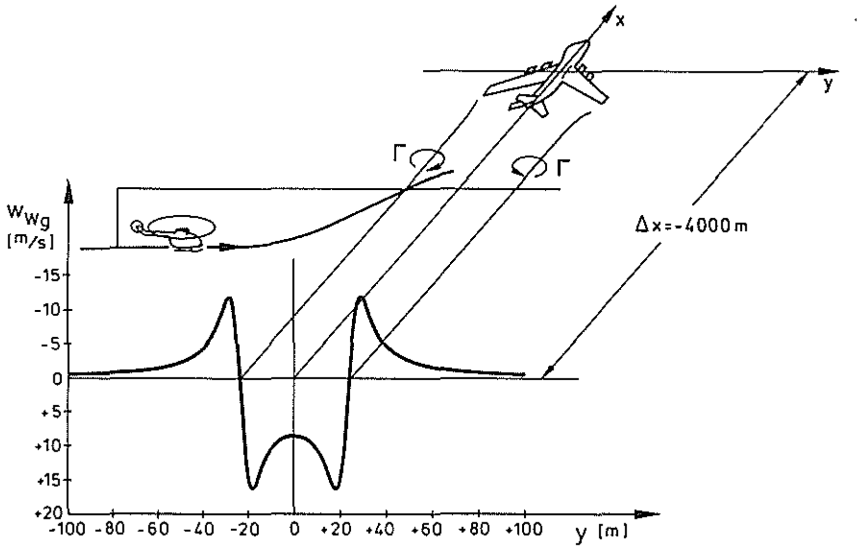

Figure 22: B 747-Trailing-Votices Penetration during Takeoff

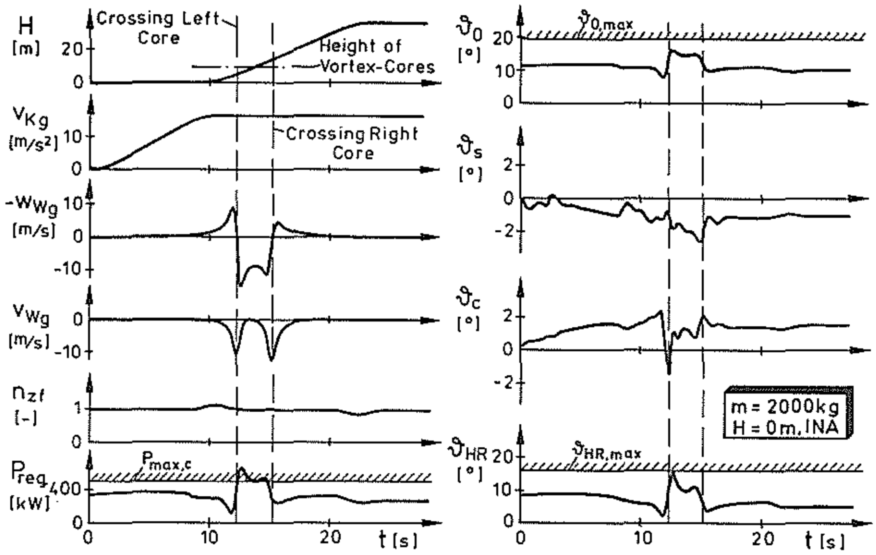

Figure 24: Normal Penetration of Trailing Vortices (x=-4000m) during Helicopter Takeoff with Defined Flight Path

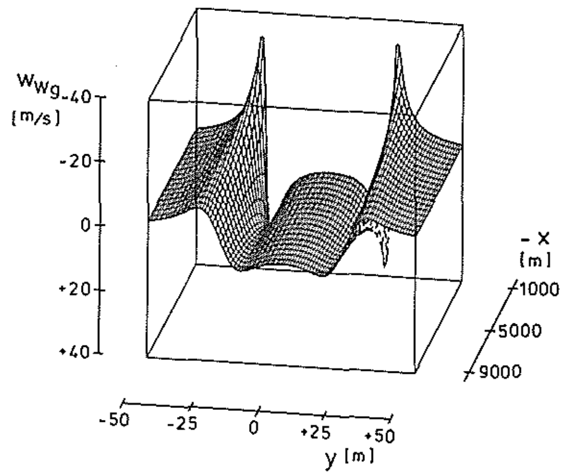

Figure 23: Induced Vertical Velocity Profile of B 747-Trailing-Vortices

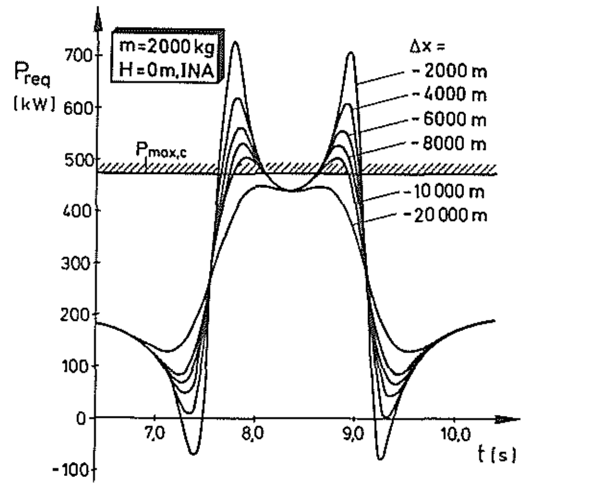

Figure 25: Normal Penetration of Trailing Vortices in Relation to Distance from Airplane